

SUPPLEMENTARY MATERIAL

This material provides additional information for the article:

An International Cohort Study of Autosomal Dominant Tubulointerstitial Kidney Disease due to *REN* Mutations Identifies Distinct Clinical Subtypes

Authors:

Martina Živná, PhD¹, Kendrah Kidd, MS^{1,2}, Mohamad Zaidan, MD, PhD³, Petr Vyleťal, PhD¹, Veronika Barešová, PhD¹, Kateřina Hodaňová, PhD¹, Jana Sovová¹, Hana Hartmannová, PhD¹, Miroslav Votruba¹, Helena Trešlová¹, Ivana Jedličková¹, Jakub Sikora¹, Helena Hůlková¹, Victoria Robins², Aleš Hnízda⁴, Jan Živný, PhD⁵, Gregory Papagregoriou, PhD⁶, Laurent Mesnard, MD⁸, Bodo B. Beck^{8,9}, Andrea Wenzel, PhD^{8,9}, Kálmán Tory, MD, PhD^{10,11}, Karsten Häeffner, MD¹², Matthias T.F. Wolf, MD¹³, Michael E. Bleyer, BS², John A. Sayer, MD PhD¹⁴⁻¹⁶, Albert C. M. Ong, DM¹⁷, Lídia Balogh, MD, PhD¹¹, Anna Jakubowska, MD, PhD¹⁸, Agnieszka Łaszkiwicz, PhD¹⁹, Rhian Clissold, MB ChB, MD²⁰, Charles Shaw-Smith, MD²⁰, Raj Munshi, MD^{21,22}, Robert M. Haws, MD²³, Claudia Izzi, MD²⁴, Irene Capelli, MD²⁵, Marisa Santostefano, MD²⁶, Claudio Graziano, MD²⁷, Francesco Scolari, MD, PhD²⁴, Amy Sussman, MD²⁸, Howard Trachtman, MD²⁹, Stephane Decramer, MD, PhD^{30,31}, Marie Matignon, MD^{32,33}, Philippe Grimbert, MD³²⁻³⁴, Lawrence R. Shoemaker, MD³⁵, , Christoforos Stavrou, MD³⁶, Mayssa Abdelwahed, PhD³⁷, Neila Belghith, MD^{37,38}, Matthew Sinclair, MD^{39,40}, Kathleen Claes, MD, PhD^{41,42}, Tal Kopel, MD⁴³, Sharon Moe, MD⁴⁴, Constantinos Deltas, PharmR, PhD⁶, Bertrand Knebelmann, MD, PhD⁴⁵⁻⁴⁷, Luca Rampoldi, PhD⁴⁸, Stanislav Knoch, PhD^{1,2}, Anthony J. Bleyer, MD, MS^{1,2}

Corresponding Author

Anthony J. Bleyer, MD, MS; Wake Forest School of Medicine; Section on Nephrology; Winston-Salem, NC, USA 27157; Fax: 336-716-4318; Phone: 336-716-4650; e-mail: ableyer@wakehealth.edu

SUPPLEMENTARY MATERIAL: Distinct subtypes of ADTKD-REN in an international cohort study

Table of Contents

Supplementary Table

Table S1. Clinical Characteristics of each ADTKD-REN mutation by Preprorenin Domain.....	3
--	---

Supplementary Figures

Figure S1. Flow diagram of the ADTKD-REN International Cohort.....	4
--	---

Figure S2. Representative family trees from 3 families with dominant <i>REN</i> mutations.....	5
--	---

Figure S3. Intracellular localization of transiently expressed mutated preprorenin, prorenin and renin in Human Embryonic Kidney 293 cells.....	6
---	---

Figure S4. Transient expression and intracellular localization of transiently expressed mutated preprorenin, prorenin and renin in Human Embryonic Kidney 293 cells (Full figure).....	7
--	---

Figure S5. Colocalization of transiently expressed mutated preprorenin, prorenin and renin in ERGIC of Human Embryonic Kidney 293 cells.....	9
--	---

Figure S6. Localization of transiently expressed mutated preprorenin, prorenin and renin in Golgi apparatus of Human Embryonic Kidney 293 cells	10
---	----

Figure S7. Localization of transiently expressed mutated preprorenin, prorenin and renin in lysosomes of Human Embryonic Kidney 293 cells	12
---	----

Supplementary Methods

Transient expression of preprorenin in HEK293 cells	14
---	----

Western blot analysis.....	14
----------------------------	----

Quantitative analysis of renin and prorenin by immunoradiometric assay (IRMA).....	16
--	----

Measurement of the enzymatic activity of renin secreted into the culture media.....	16
---	----

Confocal microscopy.....	17
--------------------------	----

Image acquisition and analysis	17
--------------------------------------	----

Supplementary References	19
--------------------------------	----

SUPPLEMENTARY MATERIAL: Distinct subtypes of ADTKD-REN in an international cohort study

Table S1. Clinical Characteristics of each ADTKD-REN mutation by Preprorenin Domain

				Presentation:									
Preprorenin Domain	REN mutation	Families	n	Acidosis, anemia, CKD	AKI	Anemia	CKD	Gout	Mean age of presentation	Anemia as a child (%)	Gout (%)	Age of first gout attack	Age of ESKD onset
Signal peptide	p.Trp10Arg	1	5	2/4 (50%)	0	2/4(50%)	0	0	15.0±11.0	5/5(100%)	1/5(20%)		46.7±14.4
	p.Leu12Pro	1	1	0	0	0	0	1/1(100%)	11	1/1(100%)	0		
	p.Leu13Gln	1	1	0	0	1/1(100%)	0	0	1.39	1/1(100%)	0		
	p.delLeu16	6	28	3/19(16%)	0	7/19(37%)	0	9/19(47%)	20.4±9.3	11/13(85%)	14/20(70%)	28±8.3	54.3±9.7
	p.Leu16Pro	3	11	1/10(10%)	1/10(10%)	0	8/10(80%)	0	19.0±16.9	6/8(75%)	7/11(64%)	30.7±13.1	45.4±10.7
	p.Leu16Arg	2	9	0	1/7(14%)	3/7(43%)	0	3/7(43%)	20.0±19.6	5/5(100%)	1/5(20%)	25	
	p. Trp17Arg	4	9	0	2/8(25%)	2/8(25%)	3/8(38%)	1/8(13%)	30.1±23.8	5/5(100%)	6/8(75%)	32.0±14.4	60.7±6.7
	p.Cys20Arg	3	5	1/5(20%)	1/5(20%)	2/5(40%)	1/5(20%)	0	11.4±11.4	5/5(100%)	2/5(40%)	29	51
Prosegment	p.Thr26Ile	2	19	0	0	4/9(44%)	0	5/9(56%)	21.4±11.7	7/10(70%)	12/16(75%)	24.9±8.4	56.0±13.0
	p. Met39Lys	1	5	0	0	3/4(75%)	1/4(25%)	0	19.5±33.1	3/3(100%)	1/4(25%)	32	32.5±24.7
	p.Glu48Lys	1	3	0	0	0	1/1(100%)	0	41	1/3(33%)	0		
Mature peptide	p.Cys325Arg	1	3	0	0	0	1/3(33%)	2/3(67%)	27.3±4.9		2/3(67%)	21±5.6	
	p.Ile366Asn	1	2	0	0	0	0	1/1(100%)	28		1/2(50%)	28	70
	p.Leu381Pro	1	5	0	0	0	2/3(67%)	1/3(33%)	51.0±10.4	0/4(0%)	1/4(25%)	45	64.0±8.2
	p.Thr391Arg	1	4	0	0	0	0	4/4(100%)	40.3±6.6	0/3(0%)	4/4(100%)	40.3±6.6	56
	p.Gln85His	1	1	0	0	0	0	1/1(100%)	20		1/1(100%)	20	

SUPPLEMENTARY MATERIAL: Distinct subtypes of ADTKD-REN in an international cohort study

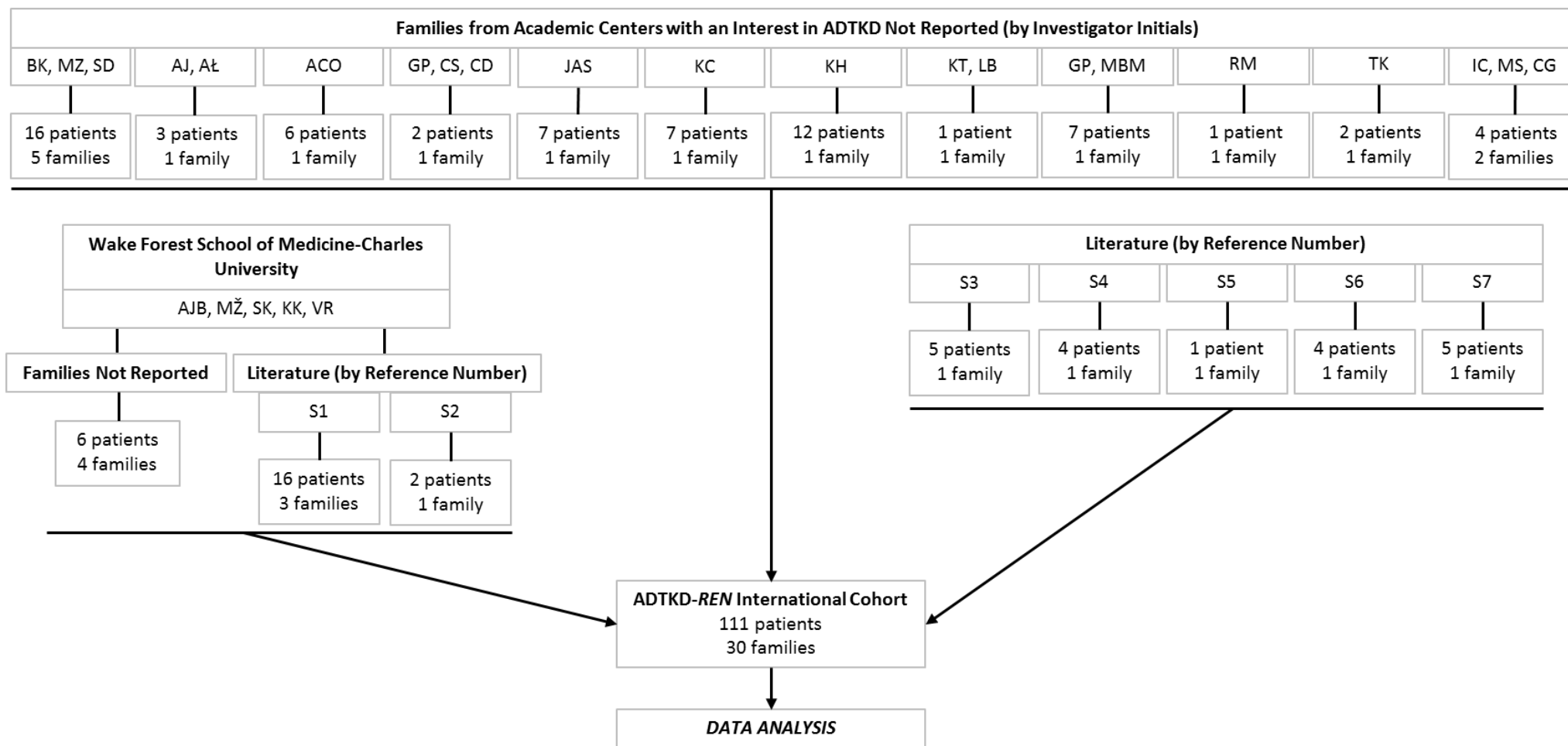


Figure S1. Flow diagram of the ADTKD-REN International Cohort. Twelve academic centers with an interest in ADTKD contributed 68 patients from 14 families previously not reported. Wake Forest School of Medicine-Charles University contributed six patients from four families previously not reported and 18 patients from four families published (S1-S2). Literature review yielded five papers describing 19 patients from five families (S3-S7).

SUPPLEMENTARY MATERIAL: Distinct subtypes of ADTKD-REN in an international cohort study

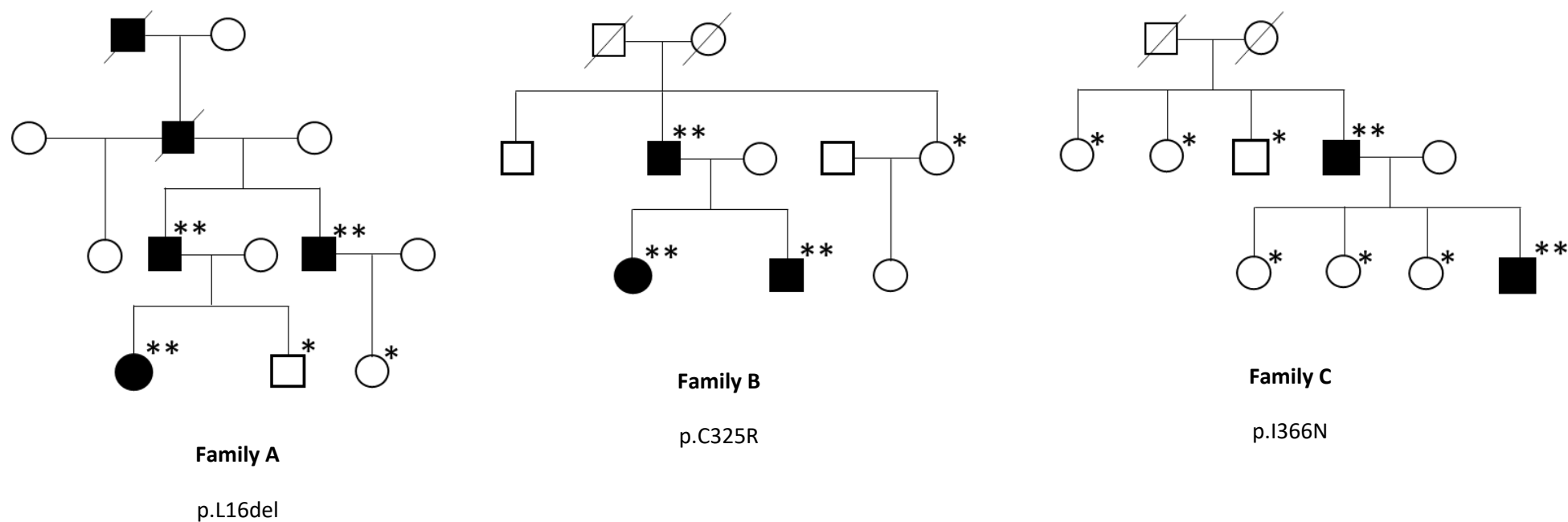


Figure S2. Representative family trees from three families with dominant *REN* mutations. Clear symbols represent clinically unaffected and filled symbols represent clinically affected. Individuals with 1 asterisk (*) underwent genetic testing and were negative. Individuals with 2 asterisks (**) underwent genetic testing and were positive for a pathogenic *REN* mutation, mutation is given below the family tree. Family trees are also found in references S1-S7.

SUPPLEMENTARY MATERIAL: Distinct subtypes of ADTKD-REN in an international cohort study

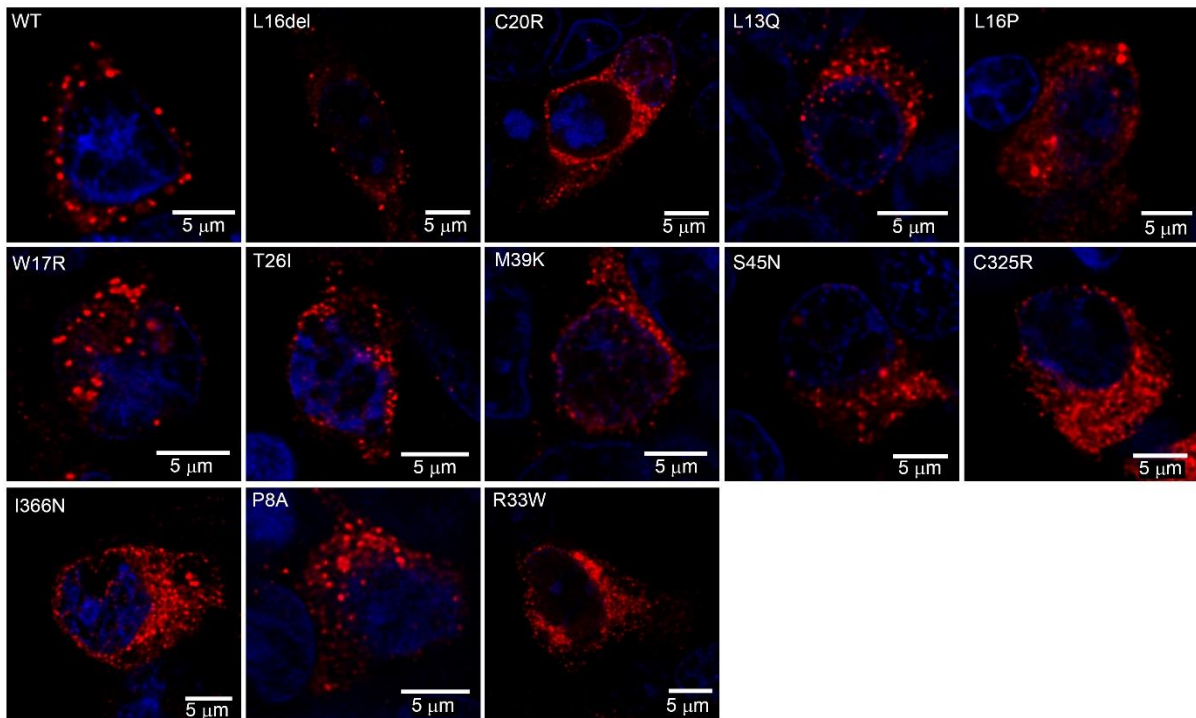


Figure S3. Intracellular localization of transiently expressed mutated preprorenin, prorenin and renin in Human Embryonic Kidney 293 cells. Immunofluorescence detection with an antibody recognizing the epitope 288-317 of preprorenin demonstrates that the wild type protein is present in coarsely granular structures that are localized exclusively in the cytoplasm. Proteins with the mutations in the signal peptide demonstrate either a very similar granular pattern (p.L16del) or intense diffuse cytoplasmic staining. Proteins with mutations in the prosegment and renin demonstrate a less distinct and more diffuse pattern.

SUPPLEMENTARY MATERIAL: Distinct subtypes of ADTKD-REN in an international cohort study

Figure S4A.

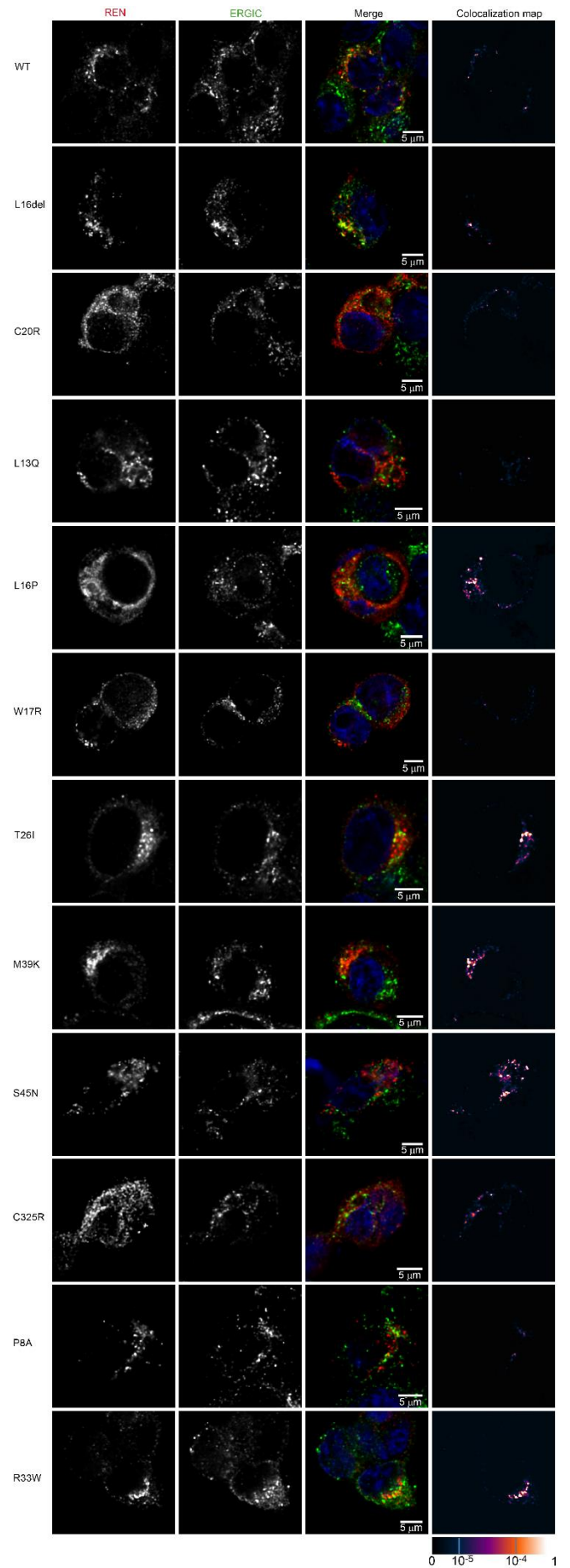


Figure S4B.

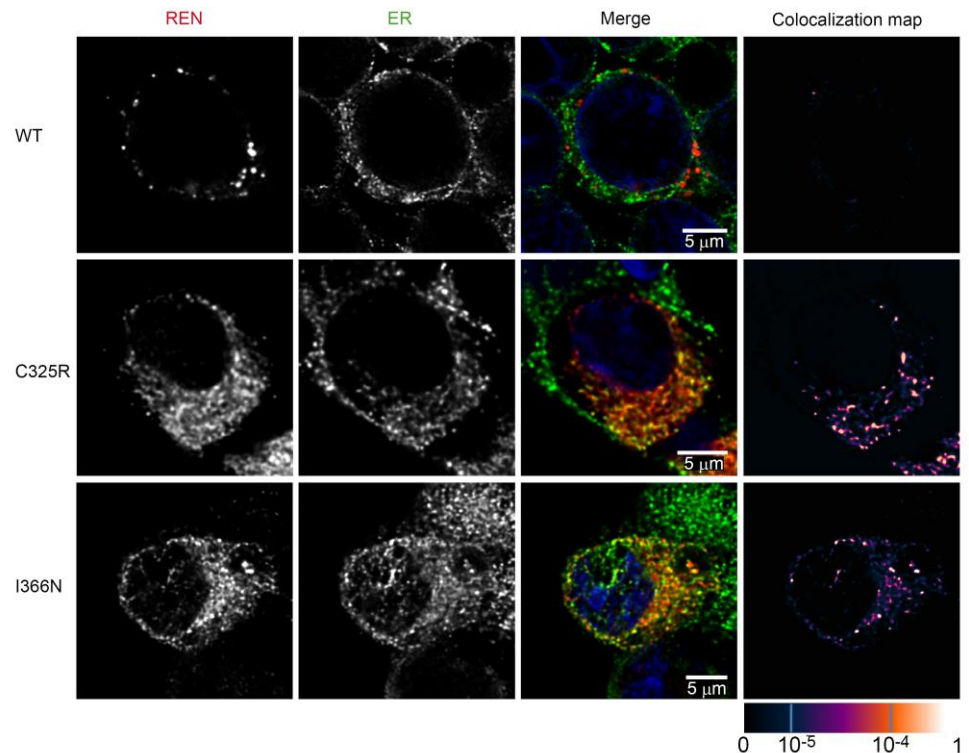


Figure S4. Transient expression and intracellular localization of transiently expressed mutated preprorenin, prorenin and renin in Human Embryonic Kidney 293 cells (Full Figure). **A.** Preprorenin, prorenin and renin were detected using an antibody recognizing the epitope 288-317 of preprorenin and co-localized with a marker of endoplasmic reticulum intermediate compartment (ERGIC53); wild type protein was present in coarsely granular structures localized exclusively in the cytoplasm. Proteins with signal peptide mutations demonstrated either a very similar granular pattern (p.L16del) or intense diffuse cytoplasmic staining; (for detailed renin staining see Supplementary Figure S3). Proteins with prosegment mutations demonstrated a less distinct and more diffuse pattern localized mainly to ERGIC. The AA_REN variant p.P8A had similar staining pattern to the wild type. The AA_REN variant p.R33W demonstrated a less distinct and more diffuse pattern localized mainly to the ERGIC. **B.** Co-staining of renin with protein disulphide isomerase (PDI), a marker of endoplasmic reticulum (ER) demonstrating localization of mature renin mutations in the ER. The degree of renin colocalization with selected markers is demonstrated by the fluorescent signal overlap coefficient values that ranging from 0-1. The resulting overlap coefficient values are presented as the pseudo color which is shown in the corresponding lookup table.

SUPPLEMENTARY MATERIAL: Distinct subtypes of ADTKD-REN in an international cohort study

Variant	Location	Pearson's coefficient	Avg	SmOdch
WT		0,18 - 0,22	0,2	0,02
L16del	SP	0,18 - 0,29	0,235	0,055
C20R	SP	0,24 - 0,37	0,305	0,065
L13Q	SP	0,27 - 0,36	0,29	0,02
L16P	SR	0,52 - 0,55	0,535	0,015
W17R	SP	0,25 - 0,31	0,28	0,03
T26I	Prosegment	0,59 - 0,72	0,675	0,085
M39K	Prosegment	0,68 - 0,76	0,72	0,04
S45N	Prosegment	0,69 - 0,84	0,765	0,075
C325R	Mature REN	0,29 - 0,36	0,325	0,035
P8A	AA_REN (SP)	0,12 - 0,32	0,22	0,1
R33W	AA_REN (Pros)	0,59 - 0,66	0,625	0,035

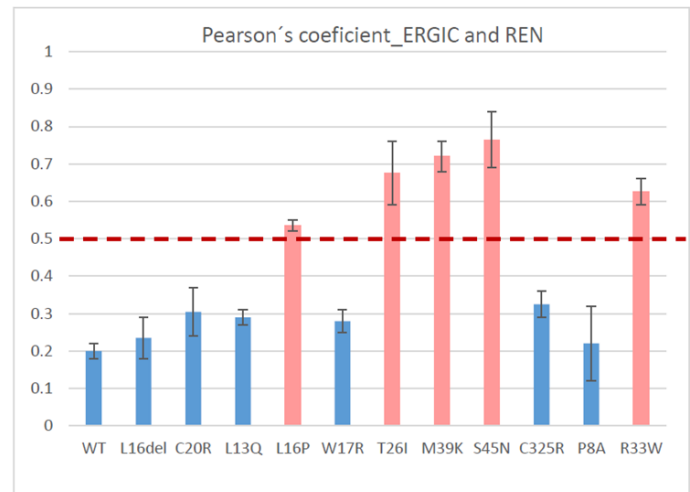


Figure S5. Colocalization of transiently expressed mutated preprorenin, prorenin and renin in ERGIC of Human Embryonic Kidney 293 cells. The Pearson's correlation coefficients of the degree of colocalization of wild type and mutated renin and ERGIC were calculated for 10 transfected cells in the Huygens Professional Software; (y-axis). A value of +1 represents perfect correlation, 0.5 random colocalization and 0 no correlation. Representative *REN* immunofluorescence staining is shown in Figure 9A and all *REN* mutations analyzed in Supplementary Figure S4A.

Figure S6.

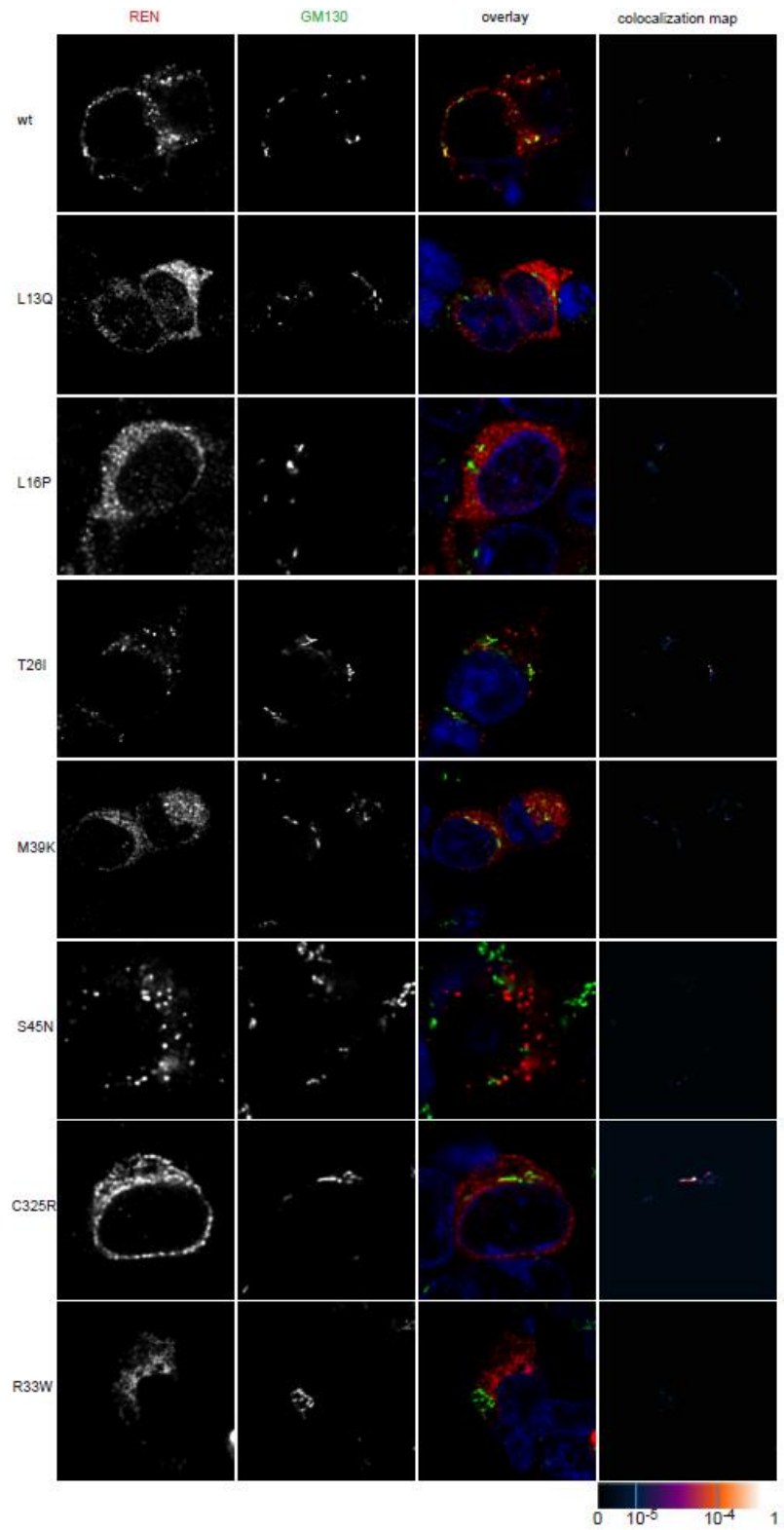
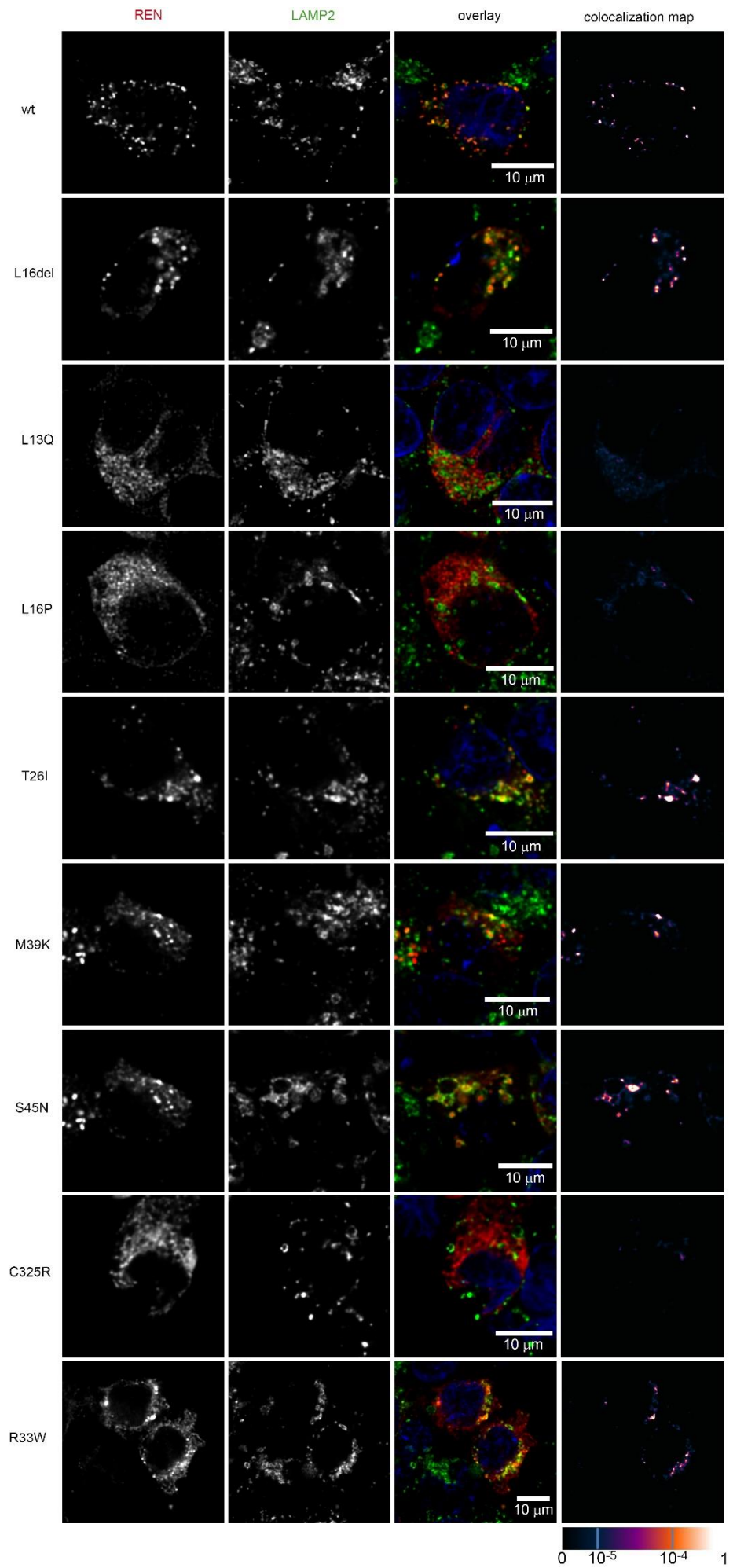


Figure S6. Localization of transiently expressed mutated preprorenin, prorenin and renin in Golgi apparatus of Human Embryonic Kidney 293 cells. Immunofluorescent costaining of renin (REN) with an antibody recognizing the epitope 288-317 of preprorenin and Golgi apparatus with mouse anti-GM130 (GM130) showing limited localization of wild type and mutant proteins in Golgi. The degree of renin colocalization with selected marker is demonstrated by the fluorescent signal overlap coefficient values that ranging from 0-1. The resulting overlap coefficient values are presented as the pseudo color which is shown in corresponding lookup table.

SUPPLEMENTARY MATERIAL: Distinct subtypes of ADTKD-REN in an international cohort study

Figure S7.



SUPPLEMENTARY MATERIAL: Distinct subtypes of ADTKD-REN in an international cohort study

Figure S7. Localization of transiently expressed mutated preprorenin, prorenin and renin in lysosomes of Human Embryonic Kidney 293 cells. Immunofluorescent costaining of renin (REN) with an antibody recognizing the epitope 288-317 of preprorenin and lysosome with Mouse anti-LAMP2 showing localization of the wild type protein, the protein with signal peptide mutation p.L16del and proteins with prosegment mutations (p.T26I, p.M39K and p.S45N) in lysosomes. Proteins with other signal peptide mutations (p.L13Q and p.L16P) and protein with mutations in the mature renin (p.C325R) did not localize to lysosomes. The degree of renin colocalization with selected marker is demonstrated by the fluorescent signal overlap coefficient values that ranging from 0-1. The resulting overlap coefficient values are presented as the pseudo color which is shown in corresponding lookup table.

SUPPLEMENTARY MATERIAL: Distinct subtypes of ADTKD-REN in an international cohort study

Supplementary Methods

Transient expression of preprorenin in HEK293 cells

8 x 10⁵ HEK 293 cells were seeded on a 6-well plate and grown for 24 hours in DMEM with 10% FCS and 1 mM HEPES (pH 7.31) containing DMEM/F12 media (Gibco) supplemented with 10% fetal calf serum (Gibco) and penicillin / streptomycin at 100 U/ml and 100 µg/ml, respectively, at 37 °C in a 5% CO₂ atmosphere (Sigma). After 24 hours, cells were transfected with Lipofectamine TM2000 with 4µg of appropriate cDNA constructs and grown either in serum-free medium without phenol red (for western blot and enzymatic activity analysis) or fully supplemented medium with phenol red (for IRMA analysis). At 24 hours after transfection, 1 mL media from each type was collected. Cells were mechanically harvested either by PBS1x for quantitative analysis of synthesized renin and prorenin (IRMA method) or lysed by lysis buffer with Protease Inhibitor Cocktail followed by qualitative study (western blot). For IRMA analysis, the amount of renin and prorenin were normalized to total protein concentration in lysates. Total protein concentration was determined using Bradford solution according to the manufacturer protocol (BioRad). Absorbance was measured by the Infinite 200 Pro reader (Tecan, Austria, GmbH) at 595 nm.

Western blot analysis

Cells cultured in FBS and phenol red-free medium were harvested to PBS and pelleted at 800g/7 min/RT. Pellets were resuspended in SDS-PAGE sample buffer (50 mM Tris HCl, 50 mM DTT, 2% SDS, pH 6,8) with Protease Inhibitor Cocktail (Sigma, Prague, Czech Republic) added in a 100:1 ratio and incubated on ice for 3 hours. Lysates were sonicated 3 times for 10 sec with an Ultrasonic Homogenizer 4710 (Cole-Palmer Instruments, Vernon Hills, IL, USA) equipped with cup horn filled with ice cold water, denatured at 100°C/5 min, cooled on ice and stored at -20°C. The protein concentration in lysates was measured by Direct Detect[®] Infrared Spectrometer (Merck Millipore, Billarica, MA, USA), according to manufacturer's instructions.

SUPPLEMENTARY MATERIAL: Distinct subtypes of ADTKD-REN in an international cohort study

For the secreted renin analysis, FBS and phenol red-free cell culture media were aspirated, mixed with a Protease inhibitor cocktail in 100:1 ratio and successively cleared at 800g/7 min and 15000g/5 min at RT. Supernatants were concentrated on Amicon® Ultra – 0.5mL Centrifugal Filters 10K (Merck Millipore, Tullagreen, Ireland) to minimal volume (about 20 µl) according to manufacturer's instructions. Concentrated media were stored at -20°C.

Volumes of lysates and media equivalent to 15 µg of proteins and 250000 cells, respectively, were mixed with 6X SDS-PAGE sample buffer (350 mM Tris Base, 10% SDS, 6% BME, 30% glycerol, 0,012% BPB, pH 6,8) in 0,2 mL tubes, denatured at 100°C/5 minutes and resolved on 4% stacking and 10% separating gel at 75 V and 150 V, respectively, in MightySmall II SE260 or SE640 apparatus (Hoefer, San Francisco, CA, USA). Proteins were then transferred to methanol-activated PVDF membrane in semi-dry blotting apparatus PHERO-Multiblot (Biotec-Fischer, Reiskirchen, Germany) at 0.6 mA/cm² for 60 minutes. Membrane was blocked in phosphate-buffered saline with 0.1% Tween 20 (PBST) and 5% BSA and probed with rabbit preprorenin (288-317) diluted 1:3000 in PBST with 0.1% BSA followed by HRP-conjugated Goat anti-Rabbit IgG (H+L) secondary antibody (Thermo Fisher Scientific, Prague, Czech Republic) at 1:10,000 dilution.

Membranes were incubated with Clarity™ Western ECL Substrate (Bio-Rad, Prague, Czech Republic) according to manufacturer's instructions. Signal was captured on CP-BU Medical X-ray blue film (Agfa) developed by Fomadent solution set (Foma Bohemia, Tisice-Chrast, Czech Republic). The tubulin protein was visualized by incubation with Mouse anti-Acetylated tubulin (T6793, Sigma Aldrich) at dilution 1:3000 in 0.1% BSA and 0.1% Tween 20 in PBS for 1 hour at RT, followed by incubation with Goat anti-Mouse HRP (Pierce) under conditions and using detection as described above.

SUPPLEMENTARY MATERIAL: Distinct subtypes of ADTKD-REN in an international cohort study

Quantitative analysis of renin and prorenin by immunoradiometric assay (IRMA)

Cell lysate was prepared as described above. The medium was centrifuged at 15,000 x g for 10 min, and the resulting supernatant was mixed with protease inhibitor cocktail in ratio 100:1 (vol/vol).

For renin determination, 50 µl of the medium and 5 µl of the lysate were diluted to a final volume of 200µl with PBS. For trypsin-activated total renin and prorenin amount, 5µl of medium and 2.5µl of lysate were incubated at 37°C for 30 min in a 50µl PBS reaction containing 100 µg and 400 µg of trypsin, respectively. The reactions were stopped by 1µl of 10 mg/mL trypsin inhibitor (PMSF, Roche, Prague, Czech Republic) and diluted to a final volume of 200 µl with PBS.

Ten µl of the resulting mixtures was mixed with 290 µl of PBS and 100 µl of the anti-hRenin (I-125) reagent (Renin III Generation Kit, CISBIO Bioassays, France), and the renin amount was measured according to manufacturer's instructions.

Measurement of the enzymatic activity of renin secreted into the culture media

We measured the enzymatic activity of renin before and after cleavage of the propeptide region and of prorenin secreted into culture media after transient expression of renin variants and wild type renin. Seeding, maintaining and transfection were performed as described above. Twenty four hours after lipofection, the medium was collected and divided into 2 tubes. Trypsin / EDTA 1x (volume ratio medium : T/E = 1: 3) was added to one tube and incubated 30 min at 37°C for cleavage of prosegment from prorenin. The trypsin reaction was stopped by adding of 2,6 µL of 50mM PMSF (Roche) and incubated for 15 min at room temperature. 100µL media before and after trypsin incubation were placed into a 96-well plate and 50µL of 100x diluted renin substrate conjugated with 5-FAM and QXL520 was added (part of Sensolyte 520 Renin Assay Kit, AnaSpec, San Jose, CA). The fluorescent signal was monitored at 528 nm every 15 min for 3 hr at 37°C on an Infinite 2000Pro microplate reader (Tecan, Austria). Each sample either before or after trypsin activation was measured in triplicate. For graph construction, we used values after 75 minutes from the start of measurement, which was the time of maximum signal in linear part of enzymatic curves.

SUPPLEMENTARY MATERIAL: Distinct subtypes of ADTKD-REN in an international cohort study

Confocal microscopy

1,5 x 10⁵ HEK293 cells were plated on polysinated glass coverslips for 24 hours and transiently transfected by LipofectamineTM3000 with 1µg plasmid DNA of wt renin, L16del, C20R, L13Q, L16P, W17R, T26I, M39K, C325R, I366N, P8A, R33W, respectively according to the manufacturer's protocol. 24 hours after lipofection, cells were quickly washed with PBS1x and fixed with cold 100% methanol. After fixing, cells were washed three times in PBS 1x and proteins were blocked for 30 min at room temperature in PBS with 5% FCS. Cells were incubated over night at 4°C with rabbit primary antibody anti-human preprorenin 288-317 (Yanaihara) at a dilution of 1:50 or mouse anti-PDI (Enzo) at a dilution 1:200 or mouse anti-ERGIC (Acris) at a dilution 1:200. For colocalization with Golgi Apparatus we used mouse anti-GM130 (ab 169276, Abcam) at a dilution of 1:300. For colocalization with lysosomes we used mouse anti-LAMP2 (H4B4) (ab 25631, Abcam) at a dilution of 1:500. Cells were washed five times in PBS 1x and incubated with donkey anti-rabbit Alexa Fluor 555 and goat anti-mouse Alexa Fluor 488 (Invitrogen) at dilution 1:1000. All antibodies were diluted in PBS 1x with 5% FCS and 0.05% Tween 20. Cells were washed four times and mounted into Antifade with DAPI (Invitrogen) for confocal imaging.

Image acquisition and analysis

Prepared slides were analyzed by confocal microscopy. XYZ images were sampled according to Nyquist criterion using a LeicaSP8X laser scanning confocal microscope, HC PL APO objective (63x, N.A. 1.40), 405, 488 and 543 laser lines. Images were restored using a classic maximum likelihood restoration algorithm in the Huygens Professional Software (SVI, Hilversum, The Netherlands). The colocalization maps employing single pixel overlap coefficient values ranging from 0-1, were created and the colocalization coefficients were calculated in the Huygens Professional Software. The resulting overlap coefficient values are presented as the pseudo color which scale is shown in corresponding lookup tables (LUT). Approximately ten cells per variant were analyzed.

SUPPLEMENTARY MATERIAL: Distinct subtypes of ADTKD-REN in an international cohort study

Supplementary References

S1. Zivna M, Hulkova H, Marignon M, et al. Dominant renin gene mutations associated with early-onset hyperuricemia, anemia, and CKD. *Am J Human Genet.* 2009;85:204-213

S2. Bleyer AJ, Zivna M, Hulkova H, et al. Clinical and molecular characterization of a family with a dominant renin gene mutation and response to treatment with fludrocortisone. *Clin Nephrol.* 2010;74:411-422

S3. Beck BB, Trachtman H, Gitman M, et al. Autosomal dominant mutation in the signal peptide of renin in a kindred with anemia, hyperuricemia, and CKD. *Am J Kidney Dis.* 2011;58:821-825.

S4. Clissold RL, Clarke HC, Spasic-Boskovic O, et al. Discovery of a novel dominant mutation in the REN gene after forty years of renal disease: a case report. *BMC Nephrol.* 2017;18:23

S5. Petrijan T, Menih M. Discovery of a Novel Mutation in the REN Gene in Patient With Chronic Progressive Kidney Disease of Unknown Etiology Presenting With Acute Spontaneous Carotid Artery Dissection. *J Stroke Cerebrovasc Dis.* 2019;28:104302.

S6. Abdelwahed M, Chaabouni Y, Michel-Calemard L, et al. A novel disease-causing mutation in the Renin gene in a Tunisian family with autosomal dominant tubulointerstitial kidney disease. *Int J Biochem Cell Biol.* 2019;117:105625.

S7. Schaeffer C, Izzi C, Vettori A, et al. Autosomal Dominant Tubulointerstitial Kidney Disease with Adult Onset due to a Novel Renin Mutation Mapping in the Mature Protein. *Sci Rep.* 2019;9:11601.